Journal of Avian Biology

JAV-02318
Redfern, C. P. F. and Bevan, R. M. 2019. Use of sea ice by arctic terns *Sterna paradisaea* in Antarctica and impacts of climate change. – J. Avian Biol. 2019: e02318

Supplementary material

Appendix 1. Electronic supplementary material

METHODS DETAIL

Stable isotope analysis

One feather from each bird was cleaned of surface contaminants using a 2M NaOH solution then rinsed in deionised water and dried overnight in an oven at 50°C. Each feather was then cut into small pieces and ~1mg was placed in a tin capsule and weighed (MT5 microbalance, Mettler). The ratios of carbon 13C:12C and nitrogen 15N:14N in the samples were measured using continuous-flow isotope-ratio mass spectrometry at The James Hutton Institute, Aberdeen, Scotland. Results are presented in δ notation relative to the international standard for PeeDee belemnite (PDB) carbonate and atmospheric N2 (air) for $\delta^{13}C$ and $\delta^{15}N$, respectively.

Midnight estimation in 24-h daylight

At or below the Antarctic Circle in the Antarctic summer, light intensity reaches a minimum at midnight, allowing longitude to be determined from the time of midnight relative to GMT. Hyperbolic curves (loglight ~ A + B * cosh(scaled time)) were fitted to light-level data within and at the boundaries of 24-h daylight as a 5-h sliding window from 5 h before the time of (daily) minimum light intensity (estimated as a 5-interval running mean as a first estimate of midnight) in 90 s steps. At each step, the time origin was set to 0 (scaled time) at the mid-point of the sliding window, representing the minimum of a hyperbolic curve, and the time step at which the residual sum of squares from a non-linear hyperbolic curve fit (function *nls* in R) reached a minimum was an estimate for midnight. This midnight estimation procedure, which finds the best minimum of a hyperbolic curve from 2.5 h before to 2.5 after the initial estimate of midnight in 90 steps, was then repeated, using the new estimates of midnight and the fitted parameters (A, B) of the hyperbolic curve, to obtain the best fitted estimate for the time of midnight. By simulation, we estimate the time of midnight to be accurate (95% confidence range) to ± 1° longitude, equivalent to ~40 km along the Antarctic Circle.

Within the light-level data for individual birds, the transition from days with night/day periods to continual daylight (but varying in intensity) was gradual and over these transition periods there were some days in which FLightR software and the midnight estimation procedure both produced longitude estimates. Because of the shallowness of the light-level curves at these transition periods, shading at critical times can markedly affect dawn/dusk threshold determination. Therefore, for merging FLightR and 24-h daylight data, longitude estimates for days with FLightR and fitted midnight estimates were assessed manually to obtain the most robust estimates of location, taking into account patterns of change in coordinate estimates by the different methods as birds entered or left 24-h daylight. For downstream analysis, the period of 24-h daylight was defined as the period for which the curve fitting technique was used to estimate longitude. An example of raw light data is shown in Fig. A1a, and a graph showing day length at different latitudes (-63° to -76° in the southern hemisphere, together with the range and median dates for entry into and exit from 24-h daylight for the sample of tagged birds as a whole, is shown in Fig. A1b.

Satellite data

Satellite data for chlorophyll-a (ocean colour) at 4 km resolution were obtained as 8-day averaged MODIS Aqua files (OCI Algorithm; mg m^{-3}; https://oceandata.sci.gsfc.nasa.gov:443/opendap/MODISA/L3SMI/). Sea Ice Concentrations (25 km resolution) were obtained as daily binary files of Nimbus-7 SMMR and DMSP SSM/I-SSMIS Passive Microwave Data (NSIDC-0051; ftp://sidads.colorado.edu/pub/DATASETS/nsidc0051_gsfc_nasateam_seaice/final-gsfc/) and were averaged into the same 8-day periods as the chlorophyll-a data. Coastline shapefiles for masking (polar stereographic projection) were 'Coastline Antarctica v02' from https://n5eil01u.ecs.nsidc.org/MEASURES/NSIDC-0709.002/. Associations between birds (either as counts per degree longitude or presence/absence) and longitude, time (expressed as 8-day periods from 1 November for each cohort), average chlorophyll-a concentration, and average sea-ice concentration, both expressed as per degree longitude within 100 km of the Antarctic coastline, were analysed in mixed-effects 'hurdle' models using the *glmmTMB* package in R (Brooks et al. 2017) with cAIC for model selection and random terms for the intercepts and slopes per bird. Similar approaches were used for analysis of sea ice concentration and chlorophyll-a at other phases within the low-temperature period. P values for the contributions of predictors to the model were estimated using the function 'mixed' in the *afex* package.

SUPPLEMENTARY TABLES

Table A1. Cohort and parameter comparisons. Statistical significance (Sig) indicated by: ns, not significant; *, 0.01 < P < 0.05; **, 0.001 < P < 0.01; ***, P < 0.001.

	Parameter	Effect	Mean: overall or 2015/2017	Median: overall or 2015/2017	Range (all)	Test[#]	n	statistic	P	Sig
a	Date, transition to low temperature	Year	7 Nov	7 Nov	20 Oct – 5 Dec	aWMW	13/24	Z= -0.844	0.4	ns
b	Date of transition from low minimum temperatures	Year	26 Mar	28 Mar	23 Feb – 12 Apr	aWMW	13/24	Z = -1.26	0.21	ns
c	Longitude at transition to low minimum temperatures	Year	111.1°[tr]	113.2°[tr]	47.0°[tr] – 177.2°[tr]	aWMW	13/24	Z= -0.67	0.5	ns
d	Latitude at transition to low minimum temperatures	Year	-48.9°	-49.6°	-64.8° – -37.4°	aWMW	13/24	Z= 1.15	0.25	ns
e	Longitude at transition from low minimum temperatures	Year	21.9°[tr]	13.7°[tr]	-22.9°[tr] – 96.2°[tr]	aWMW	12/24	Z= -0.34	0.74	ns
f	Latitude at transition from low minimum temperatures	Year	-61.6°	-64.4°	-75.6° – -36.9°	aWMW	12/24	Z= 1.07	0.28	ns
g	Longitude at start (row c) & end (row e) of low temperature period	Difference End-start	n/a	n/a	n/a	WRS	37/36	W= 39	<<0.0001	***
h	Latitude at start (row d) & end (row f) of low temperature period	Difference End-start	n/a	n/a	n/a	WRS	37/36	W= 164	<0.0001	***
i	Latitude with time in pre-Antarctic low-temperature zone, 8-day periods	Year (main effect)	Coefficient: 0.21	n/a	n/a	LME[¶]	461/694	$F_{1/34.7}$=4.1	0.049	*
j	Date before 24-h daylight	Year	22 Nov	22 Nov	7 Nov – 5 Dec	aWMW	23/24	Z = 1.87	0.062	.
k	Latitude before 24-h daylight	Year	-62.3° / -64.9°	-63.6° / -64.8°	-43.7° – -68.5°	aWMW	23/24	Z = 2.75	0.006	**
l	Longitude before 24-h daylight	Year	113°[tr]	106.9°[tr]	1.8°[tr] – 237.7°[tr]	aWMW	23/24	Z= -0.12	>0.9[¶¶]	ns
m	Longitude at last FLightR estimate and first 24-h daylight[¶¶¶]	Difference[‖]	-2.6°[tr]	n/a	95% CI: -4.2°[tr] – -1.0°[tr]	1n-t.test	47	t= -3.3	0.002	**
n	Duration of 24-h daylight phase	Year	70 days	67 days	55 – 105 days	aWMW	22/24	Z= 0.53	0.6	ns
o	Longitudinal movement in 24-h daylight	Difference: end - start	24.1°[tr] (mean difference)	20.4°[tr] (median difference)	-24.8°[tr] – 93.3°[tr] (difference range)	WSR	46	V= 1005	<0.0001	***
p	Intercepts: first-order longitude versus time in 24-h daylight[¶¶¶¶]	Year	119.8°[tr] / 120.1°[tr]	114.9°[tr] / 120.8°[tr]	21.1°[tr] – 241.7°[tr]	aWMW	23/24	Z= 0.17	0.86	ns
q	Slopes: first-order longitude versus time in 24-h daylight[¶¶¶¶]	Year	-0.54 / -0.24	-0.4 / -0.1	-1.6 – 0.36	aWMW	23/24	Z= -2.17	0.03	*
r	Date at end 24-h daylight	Year	31 Jan	29 Jan	18 Jan – 24 Feb	aWMW	22/24	Z= 1.5	0.13	ns

s	Longitude at end 24-h daylight	Year	90.4°[tr]	93.7°[tr]	-36.6°[tr] – 197.8°[tr]	aWMW	22/24	Z ≤ -1.2	>0.15¶¶	ns
t	Latitude at end 24-h daylight	Year	-67.2°	-66.5°	-76.4° – -63.7°	aWMW	22/24	Z= -0.35	> 0.7	ns
u	Latitudes and end 24-h daylight	Correlation				S'man	46	R= -0.78	< 0.0001	***
v	Days end 24-h daylight to end of low-temperature period	Year	55.4	60	20 – 78 days	aWMW	13/24	Z= -0.86	0.39	ns
w	Ice and chlorophyll-a at locations between 24-h daylight and departure	Correlation	0.33 $mg.m^{-3}$	0.19 $mg.m^{-3}$	0.02 – 3.47 $mg.m^{-3}$	S'man	2132	R= -0.1	< 0.0001	***

[#]aWMW, asymptotic Wilcoxon-Mann-Whitney; LME, linear mixed effects; WSR, Wilcoxon-signed-rank; WRS, Wilcoxon Rank Sum; 1n-t.test, 1-sample t-test; S'man, Spearman.

[°tr] Transformed longitude scale (-50° to 260°); 197.8 is equivalent to -162.2° longitude.

[¶] ANOVA, Box-Cox transformation of latitude, linear mixed-effects 2[nd]-order polynomial with respect to time period; year as a main effect and interaction; time: $F_{2,1138.8}$=225.4, P < 0.00001; interaction with year: $F_{2,1138.8}$=8.6, P < 0.0002).
[¶¶]with or without re-tagged birds.

[¶¶¶]This is the difference between the last FLightR estimate of longitude and the first curve-fitted estimate of longitude the following day and suggests a slight easterly trajectory as birds complete their move towards the Antarctic Circle. There was no significant difference between years, aWMW, Z = 1.4, P = 0.16.

[¶¶¶¶] First-order linear models were fitted to longitude trajectories[°tr] with respect to day (date) in 24-h daylight; intercepts can be viewed as proxies for longitude at entry into 24-h daylight and slopes as comparators for the scale of movement with time.

Table A2. Repeatability. Statistical significance (Sig) indicated by: ns, not significant; *, 0.01 < P < 0.05; **, 0.001 < P < 0.01; ***, P < 0.001

Row	Parameter	sample	Repeatability[#]	P	Sig
a	Date of transition to low minimum temperatures	7[¶]	0.43	0.116	ns
b	Date of transition from low minimum temperatures	6[¶]	0	0.5	ns
c	Longitude[°tr] at transition to low minimum temperatures	7[¶]	0.419	0.122	ns
d	Latitude at transition to low minimum temperatures	7[¶]	0.298	0.21	ns
e	Longitude[°tr] at transition from low minimum temperatures	6[¶]	0.472	0.11	ns
f	Latitude at transition from low minimum temperatures	6[¶]	0.303	0.224	ns
g	Date of entry to 24-h daylight	10	0.504	0.042	*
h	Latitude before 24-h daylight	10	0.224	0.24	ns
i	Longitude[°tr] before 24-h daylight	10	0.67	0.007	**
j	Longitude[°tr] at arrival in 24-h daylight	10	0.705	0.004	**
k	Duration of 24-h daylight phase	10	0.322	0.148	ns
l	Longitudinal[°tr] movement around Antarctic	10	0	0.5	ns
m	Intercepts; first-order longitude[°tr] versus time in 24-h daylight[¶¶]	10	0.7	0.005	**
n	Slopes; first-order longitude[°tr] versus time in 24-h daylight[¶¶]	10	< 0.1	0.5	ns
o	Date at end of 24-daylight	10	0	0.5	ns
p	Longitude[°tr] at end of 24-h daylight	10	0.509	0.042	*
q	Latitude at end of 24-h daylight	10	0	0.5	ns
r	days end 24-h daylight to end of low-temperature period	6[¶]	0	0.5	ns

[#]range 0 (none) to 1 (highly repeatable).
[°tr] Transformed longitude scale (-50° to 260°).
[¶] Sample size was reduced with respect to temperature analyses because some geolocators used in 2015 were programmed in 'clipped mode' which does not record temperature.
[¶¶] As in Table 1, intercepts from first-order linear models fitted to longitude trajectories[°tr] can be viewed as proxies for longitude at entry into 24-h daylight and slopes as comparators for the scale of movement with time.

Table A3: We asked whether the presence and number of tagged birds was predicted by seasonal progression (8-day periods from 1 November), sea ice concentration and/or chlorophyll-a concentration within 100 km (diameter of assumed geolocation-point accuracy) of the coast at East Antarctic longitudes 45° to 155° during the 24-h daylight phase. These relationships were tested using a mixed-effects generalised linear 'hurdle' model (Brooks et al. 2017) on the number (count; conditional on ice, chlorophyll-a, and time period) and absence (zero-inflated model; predicted by the variables in the model) of geolocator birds in each longitude interval. In the model, bird (intercept) and slope (time) per bird were included as random effects; cohort (year), either as a random or fixed effect was not significant, did not appear in the top models selected by AIC and was not included in the final model set. In the top model after model selection on ΔAIC, ice concentration was additive with chlorophyll and time-period as interactive effects. Statistical significance (Sig) indicated by: ns, not significant; . , 0.05 < P < 0.1; *, 0.01 < P < 0.05; **, 0.001 < P < 0.01; ***, P < 0.001

a. **Model selection**: all generalised linear 'hurdle' models were zero-inflation for all effects with truncated negative binomial-2¶ distribution.

Fixed effects	df	ΔAIC
ice + chlorophyll * period	15	0
ice	9	2.9
ice * chlorophyll * period	21	8.1
chlorophyll * period	13	32.5
chlorophyll	9	46.7
chlorophyll + ice * period	15	100.1

¶variance increases quadratically with mean.

b. **Top model**: count ~ ice + chlorophyll * period; zero-inflation for all effects in model, family= truncated negative binomial (variance increases quadratically with mean); AIC, 27422.0; log Likelihood, -13696.0; deviance, 27392.0; residual df, 86460.

Random effects; overdispersion parameter: 4.12; observations 86475; groups 44.

Model	Group	Parameter	Variance	SD
Conditional	bird	Intercept	0.02567	0.1602
	bird	Period (slope)	0.01208	0.1099
zero -inflated	bird	Intercept	0.22827	0.4778
	bird	Period (slope)	0.04619	0.2149

Fixed effects

Model	Parameter	Coefficient	SE	Z	P (> |Z|)	Sig
Conditional	Intercept	-0.58	0.09	-6.62	< 0.0001	***
	ice	-0.1	0.04	-2.37	0.0177	*
	chl	-0.09	0.05	-1.77	0.0774	.
	period	-0.06	0.05	-1.09	0.2779	ns
	chlorophyll*period	0.06	0.06	1.09	0.2745	ns
zero -inflated¶¶	Intercept	3.48	0.08	45.93	< 0.0001	***
	ice	-0.01	0.02	-0.56	0.5776	ns
	chl	-0.1	0.02	-4.80	< 0.0001	***
	period	0.08	0.04	1.87	0.0615	.
	chlorophyll*period	0.29	0.02	11.79	< 0.0001	***

¶¶Unlike a conventional binomial model, the zero-inflated component of the 'hurdle model' tests for probability of zero in relation to effects in the model. Therefore, the probability of zero decreases as chlorophyll increases.

Table A4: Change in the presence of ice (a, generalised mixed-effects binomial model) or chlorophyll-a concentrations (b, linear mixed effects model) at bird locations with time period during the post-24-h daylight phase, 8-day periods, grouped from 1 January. Statistical significance (Sig) indicated by: ns, not significant; . , 0.05 < P < 0.1; *, 0.01 < P < 0.05; **, 0.001 < P < 0.01; ***, P < 0.001

a. Model: Linear mixed effects; chlorophyll-a (Box-Cox transformation) ~ period; observations, 2132; birds 36.

Random effects;

Group	Parameter	Variance	SD
bird	Intercept	2.2e-02	0.15
bird*period	Slope	7.3e-05	0.009
	Residual	6.4e-04	0.025

Fixed effects

Parameter	Coefficient	SE	df	t	P (> |t|)	Sig
Intercept	0.81	0.03	33.7	30.98	< 0.0001	***
Period	0.002	0.001	33.3	1.14	0.263	ns

b. Model: generalised binomial linear mixed effects; ice ~ period; AIC, 20175.0; log likelihood -1033.5; deviance, 2067.0; residual df, 2128; observations, 2132; birds 36.

Random effects;

Group	Parameter	Variance	SD
bird	Intercept	349.135	18.685
bird*period	Slope	1.091	1.044

Fixed effects

Parameter	Coefficient	SE	Z	P (> |Z|)	Sig
Intercept	8.97930	3.55794	2.524	0.0116	*
Period	0.04458	0.18571	0.240	0.8103	ns

Table A5: Count (dependent variable) of tagged bird locations in relation to modelled (Bestley et al. 2018) Krill swarm density. The generalised linear mixed-effects 'hurdle' models incorporate 'bird' as a random factor (intercept). Statistical significance (Sig) indicated by: ns, not significant; . , 0.05 < P < 0.1; *, 0.01 < P < 0.05; **, 0.001 < P < 0.01; ***, P < 0.001

a. Model selection

Fixed effects	Model	df	ΔAIC
krill	zero-inflation, all effects in model; family= truncated negative binomial-2¶	7	0
krill	zero -inflation, all effects in model; family= truncated negative binomial-1¶	7	27.4
1	zero -inflation, all effects in model; family= truncated negative binomial-2 [null model]	5	207.6
krill	zero -inflation, all effects in model; family= truncated Poisson	6	1118.4
krill	zero -inflation probability equal for all cells; family= Poisson,	4	1451.2

¶ truncated negative binomial-1: variance increases linearly with mean; truncated negative binomial-2: variance increases quadratically with mean.

b. Top model: count ~ krill; zero -inflation for all effects in model, family= truncated negative binomial (variance increases quadratically with mean); AIC, 11812.6; log Likelihood, -5899.3; deviance, 11798.6; residual df, 1551251.

Random effects; overdispersion parameter: 8.99e-09; observations: 1551258; groups: 46

Model	Group	Parameter	Variance	SD
Conditional	Bird	Intercept	0.75	0.87
zero -inflated	Bird	Intercept	0.79	0.89

Fixed effects

Model	Parameter	Coefficient	SE	Z	P (> |Z|)	Sig
Conditional	Intercept	-16.9	1428	-0.012	> 0.9	ns
	Krill	-0.005	0.0086	-0.58	0.57	ns
zero -inflated¶¶	Intercept	8.78	0.15	58.27	<< 0.0001	***
	Krill	-0.053¶¶	0.003	-17.79	<< 0.0001	***

¶¶Unlike a conventional binomial model, the zero-inflated component of the 'hurdle model' tests for probability of zero in relation to krill swarm density. Therefore, the probability of zero decreases as krill swarm density increases.

SUPPLEMENTARY FIGURES

Fig. A1 a, A 'lightImage' plot of the raw (log-transformed) light data from a bird in the 2015 cohort to show the transitions to and from 24-h daylight. This bird (G82) travelled the furthest (see Fig. A7), and the shift in time of midnight relative to GMT was about 16 h, representing a movement of ~240° longitude. **b**, Plots of day length (ordinate, h) by date (day of the year) at latitudes from -63° to -76° in 1° intervals (grey lines); the red plot is day length at the Antarctic Circle (-66.56°). The horizontal blue line is 24-h daylight; black arrows above this line represent the date (day of the year) of the earliest and latest entry/exit from 24-h daylight from geolocator data, with median dates represented by green arrows. The graph was constructed with the *insol* package in R. **c**, Example of changepoint analysis to define objectively the start and ends of the low-temperature period. In this profile, a bird from the 2015 cohort, vertical grey dashed lines mark changepoints identified by the software package; the two marked in blue were defined as the start (left line) and end (right line) of the low temperature period. Date is shown on the abscissa. For all data during the low temperature period defined by the change points, the temperature range was -9 to 10° C with mean/median of -2.3° C (sd 1.44, n=5158).

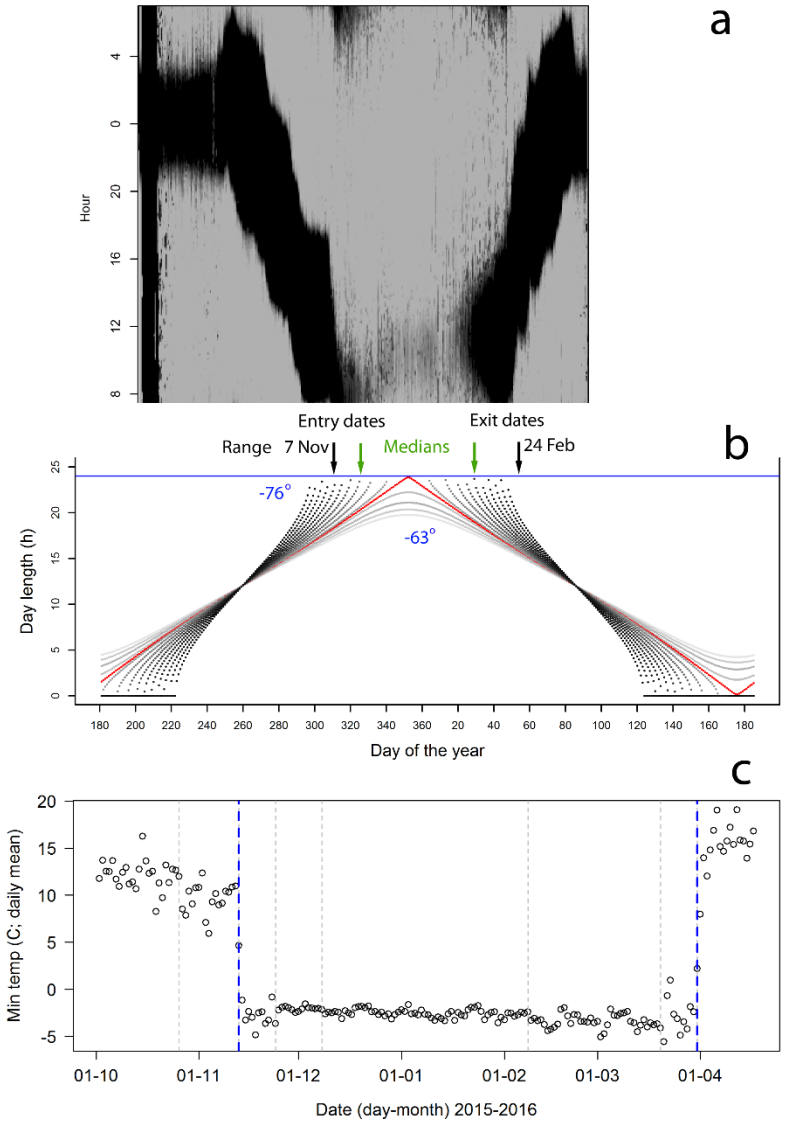

Fig. A2 Additional data for bird locations between the start of the low-temperature zone to start of 24-h daylight in 8-day periods, overlaid onto satellite data for sea ice concentration (percentage; linear gradient: <1% [blue] to 100% [white]; colour gradient legend in centre). Red symbols are geolocations for individual birds, with a different symbol style for each individual. Longitudes are in 20° intervals, and three latitudes are given: -66.56° (Antarctic Circle), -73.3° and -80°. Ice concentrations are means of the daily ice-concentration data for the relevant 8-day periods.

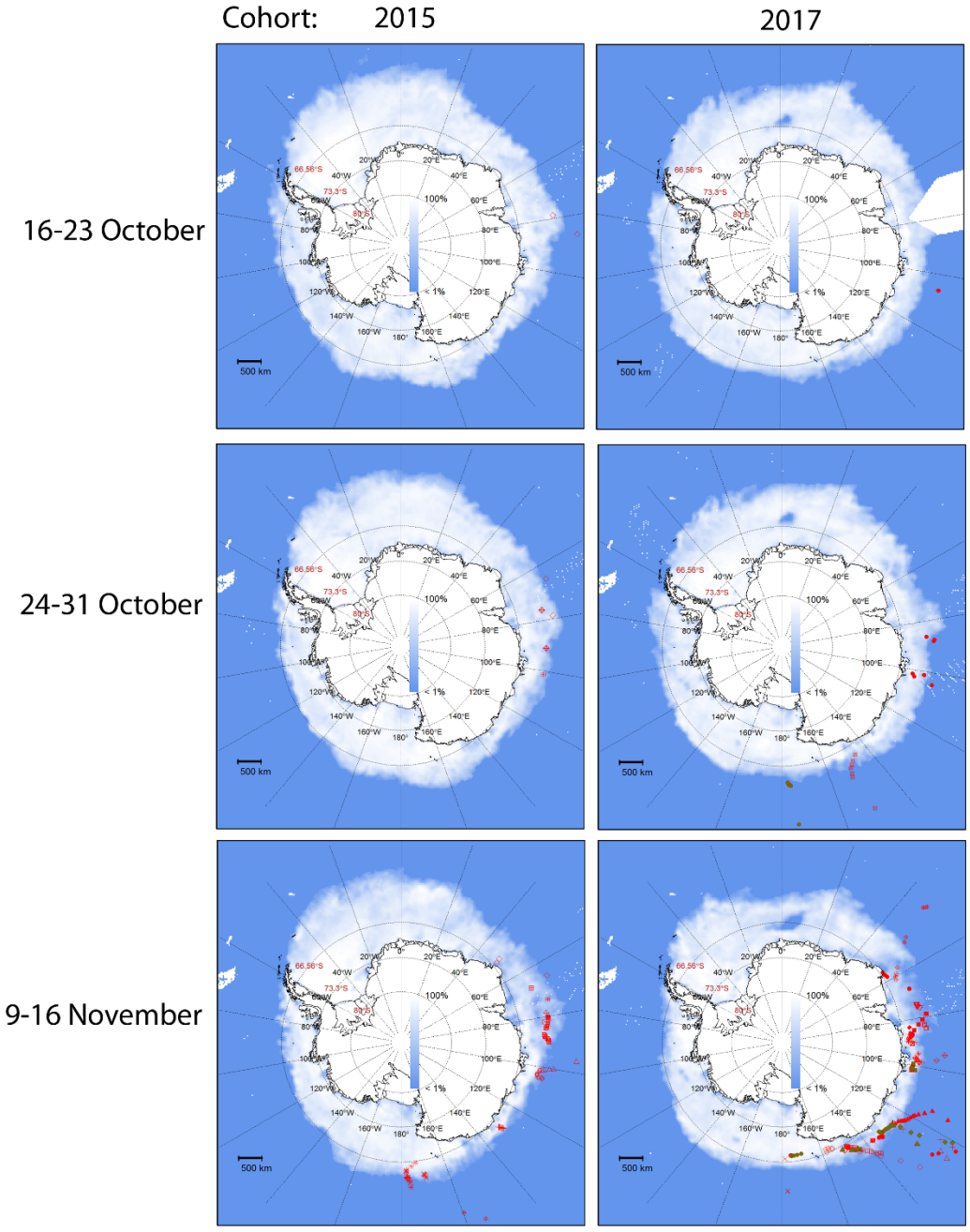

Cohort: 2015 2017

25 November -2 December

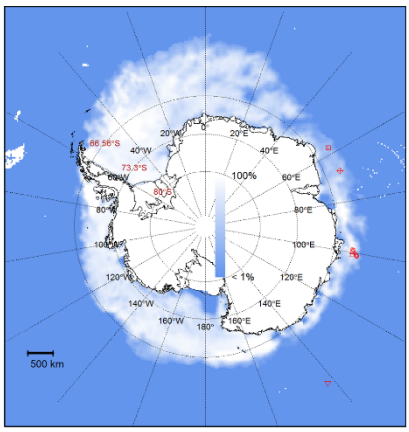

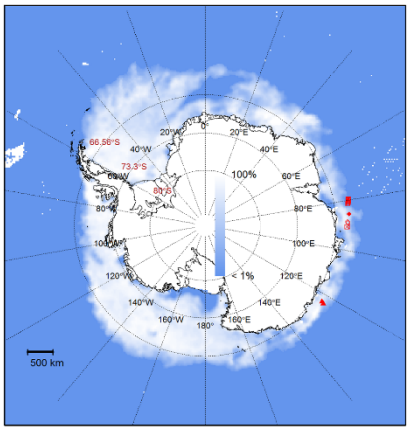

3-10 December

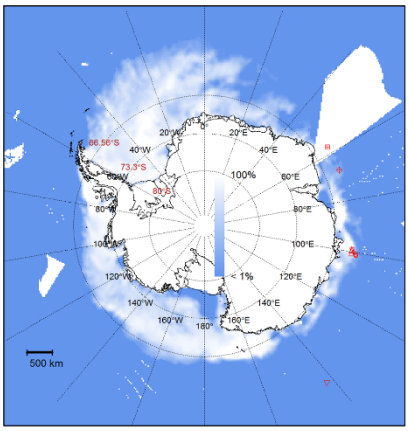

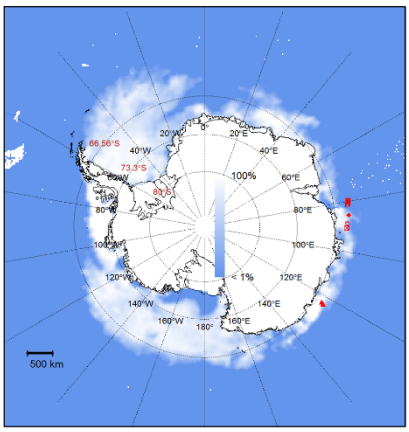

Fig. A3 Longitude trajectories of re-tagged birds in 24-h daylight in 2015 and 2017. The same colour is used for the same individual in both years. The longitude scale has been transformed from 0° – 180°, -180° – 0° to a continuous linear scale from -50° to 260° with 0 at the Greenwich Meridian. The abscissa is days from the start day for the relevant year. Second-order curves were fitted to each bird to illustrate trajectories.

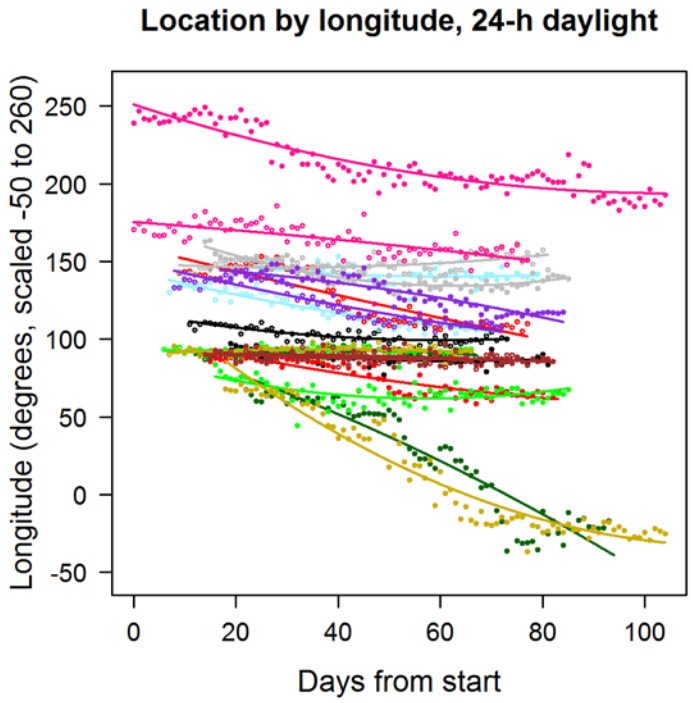

Fig. A4 Antarctic geolocator positions in relation to sea-ice concentration in the low temperature period after the end of the 24-h daylight phase- additional data for the 2015 cohort in the same period in 2016 as shown in Fig. 3, and the remaining data for the 2017 cohort in 2018.

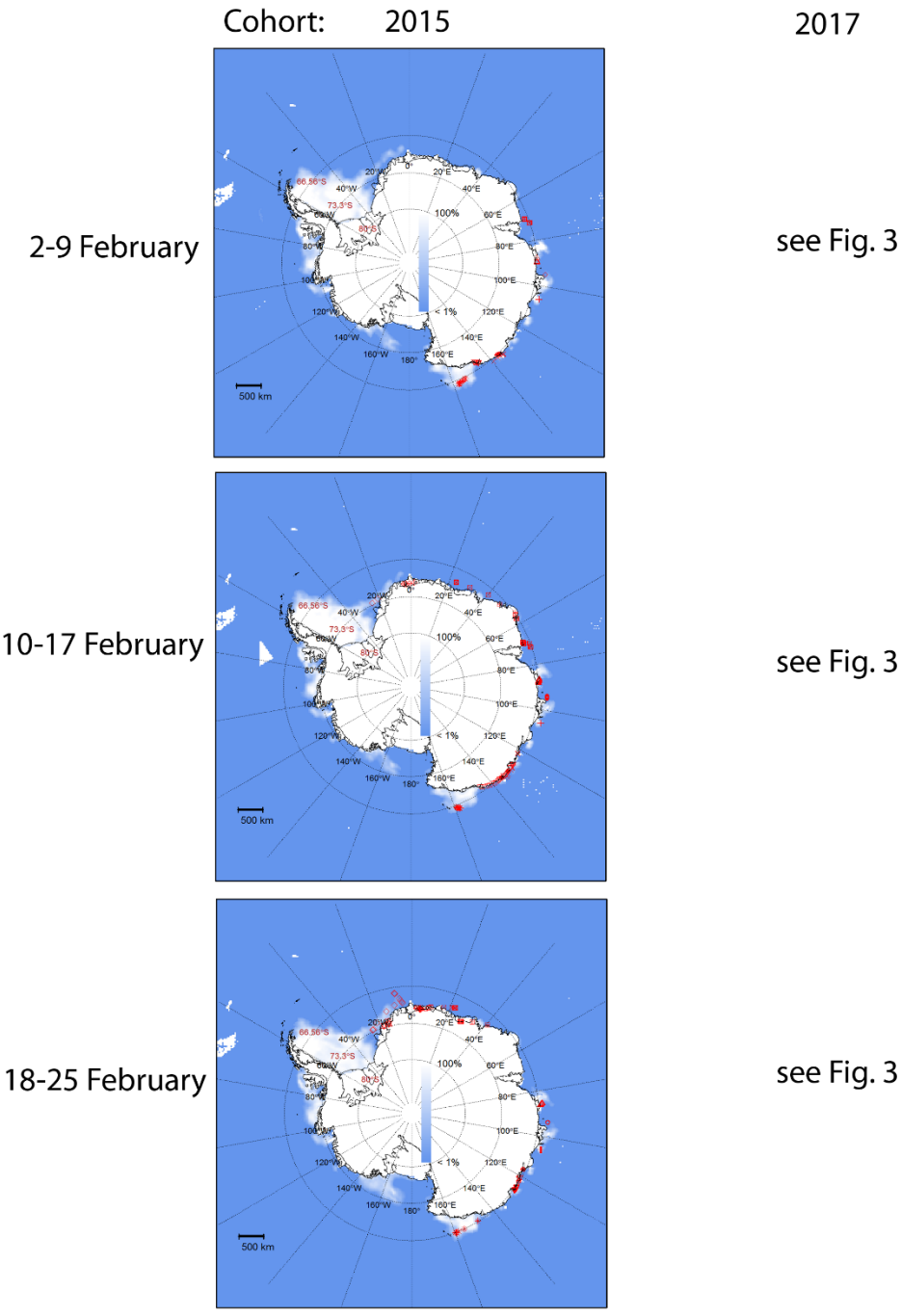

Cohort: 2015 2017

26 February -5 March

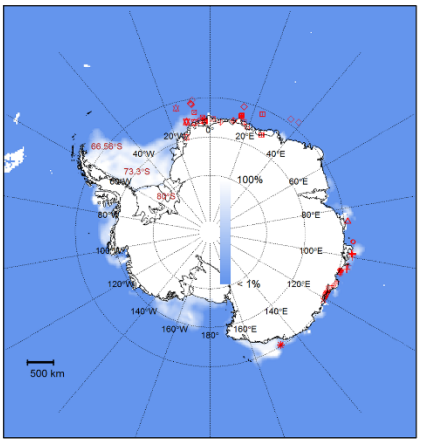

see Fig. 3

6-13 March

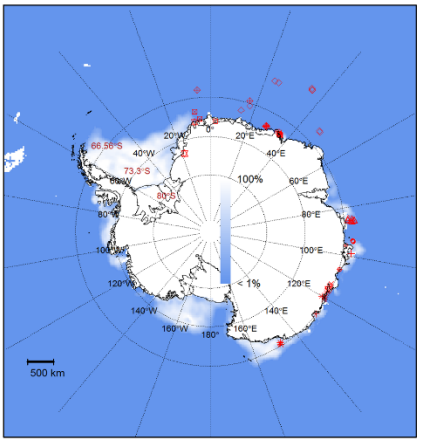

see Fig. 3

14-21March

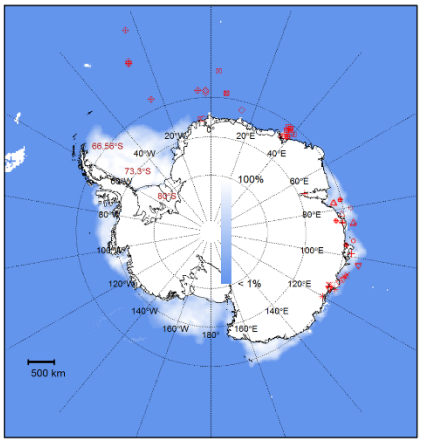

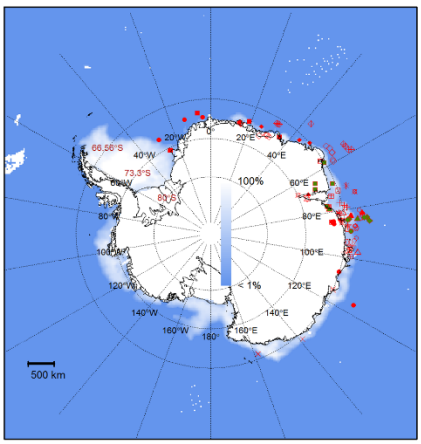

Cohort: 2015 2017

22-29 March

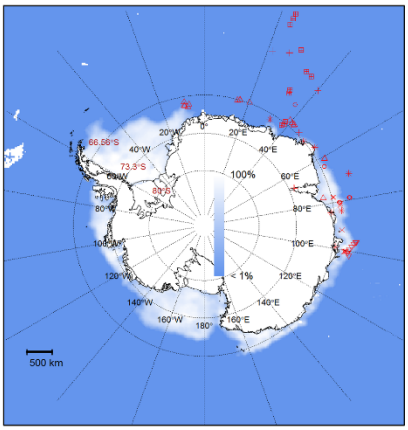

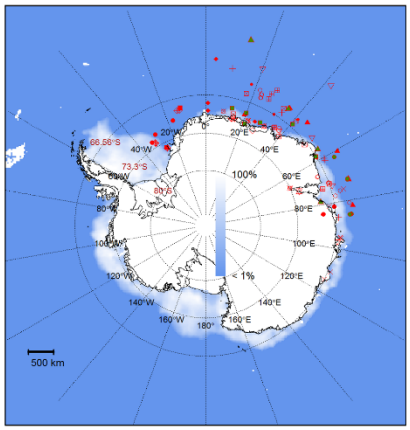

30 March
-6 April

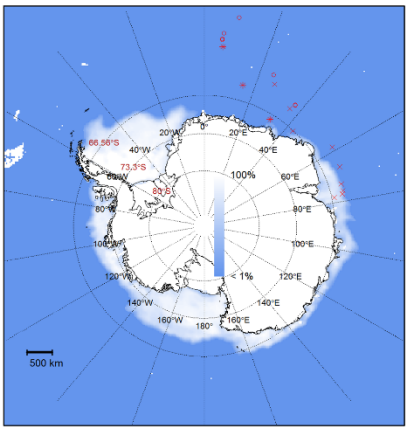

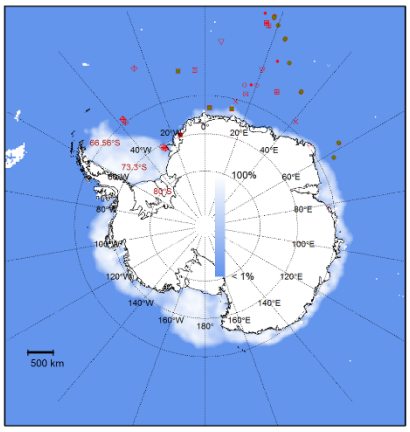

7-14 April

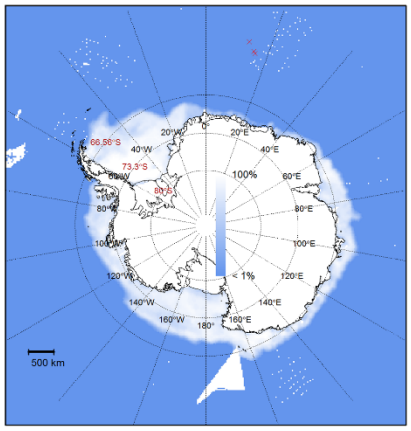

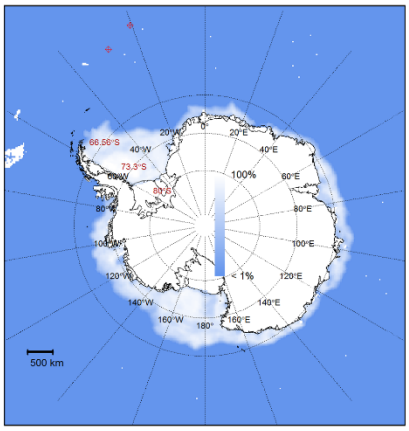

Fig. A5 Mean daily movement speeds (m.s^{-1}, ordinate axes) for each bird from 1 November in 2015 (a) and 2017 (b, c) used for analysis of geolocation between the end of 24-h daylight and end of the low temperature zone. Colours indicate phases within the low-temperature period as defined in the legend to Fig.1. Data for 12 birds are shown in each panel. The sample size for 2015 is 12 birds because the geolocators used for the other birds were programmed in a 'clipped' mode which does not record temperature and a low temperature zone cannot be defined for those birds which have therefore been omitted.

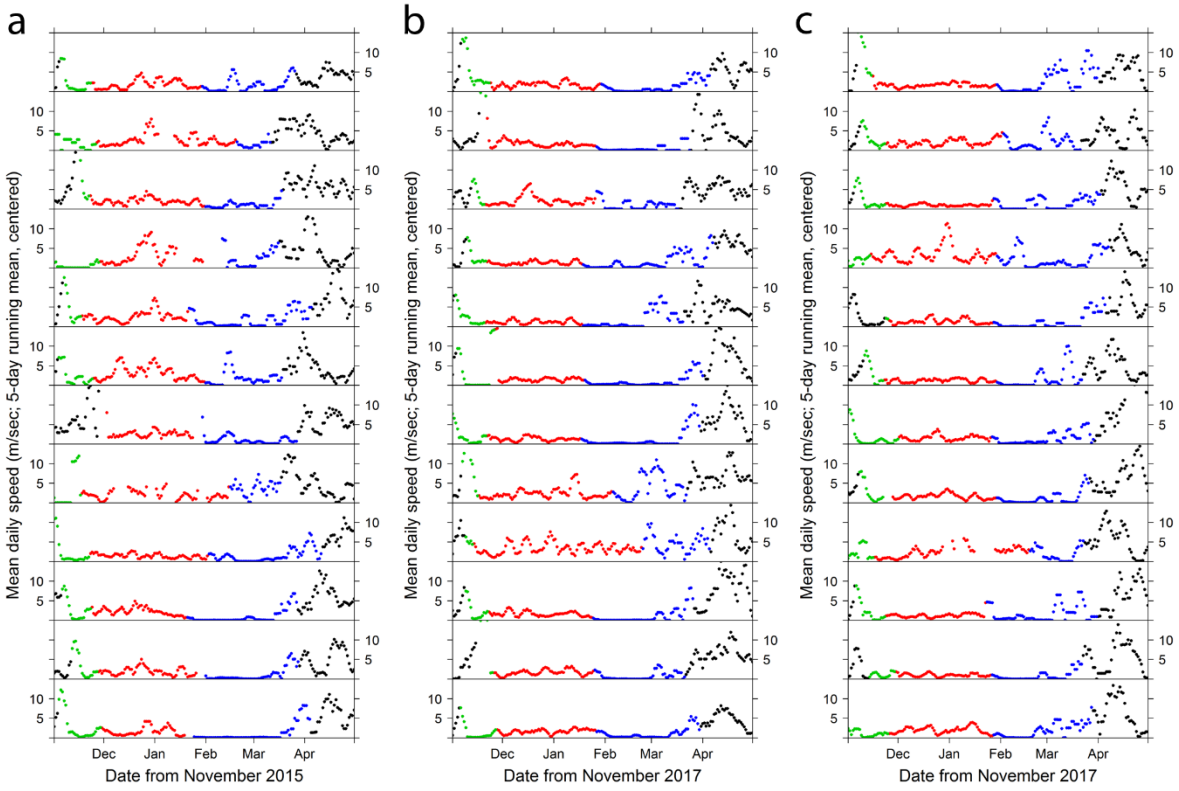

Fig. A6 Longitude trajectories of re-tagged birds after the 24-h daylight phase and at latitudes less than -60°. The abscissas and longitude scales are as described in Fig. 5. All geolocations were with FLightR and the lines fitted to summarise the movement trends are 3rd-order polynomials to capture the greater complexity of movement compared to the 24-h daylight phase. For birds in 2017, all points were defined by and within the interval between the end of 24-h daylight and the end of the low-temperature period. This also applies to 12 birds with loggers in the full recording mode in 2015, but data for the other loggers in clipped recording mode in 2015 have also been added, and for these birds the constraint is latitude only (less than -60°) rather than latitude and time with respect to the low temperature period. The same colour is used for re-tagged birds in 2015 and 2017.

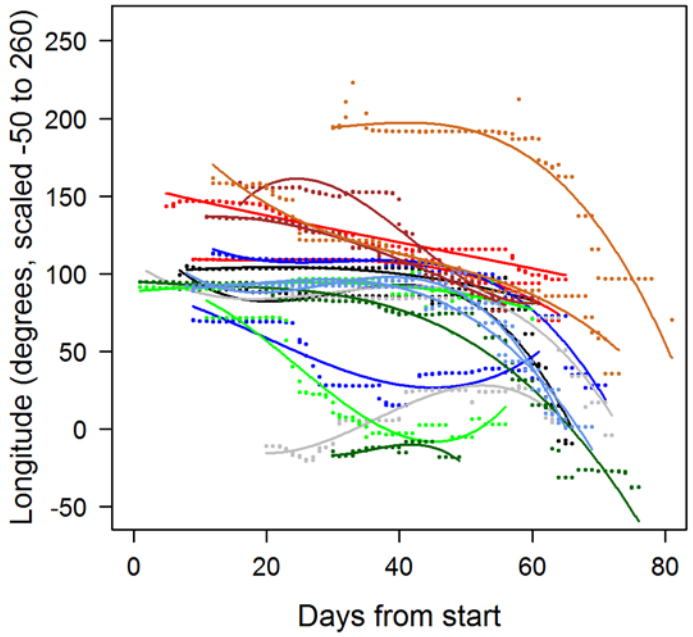

Fig. A7 Inferred movement trajectories in the Antarctic for birds tagged in 2015 (red 'tracks'and again in 2017 (blue 'tracks'). Open circles (larger diameter than the filled symbols for FLightR geolocations) are used for the daylight phase where longitudes were estimated using the curve-fitting procedure.

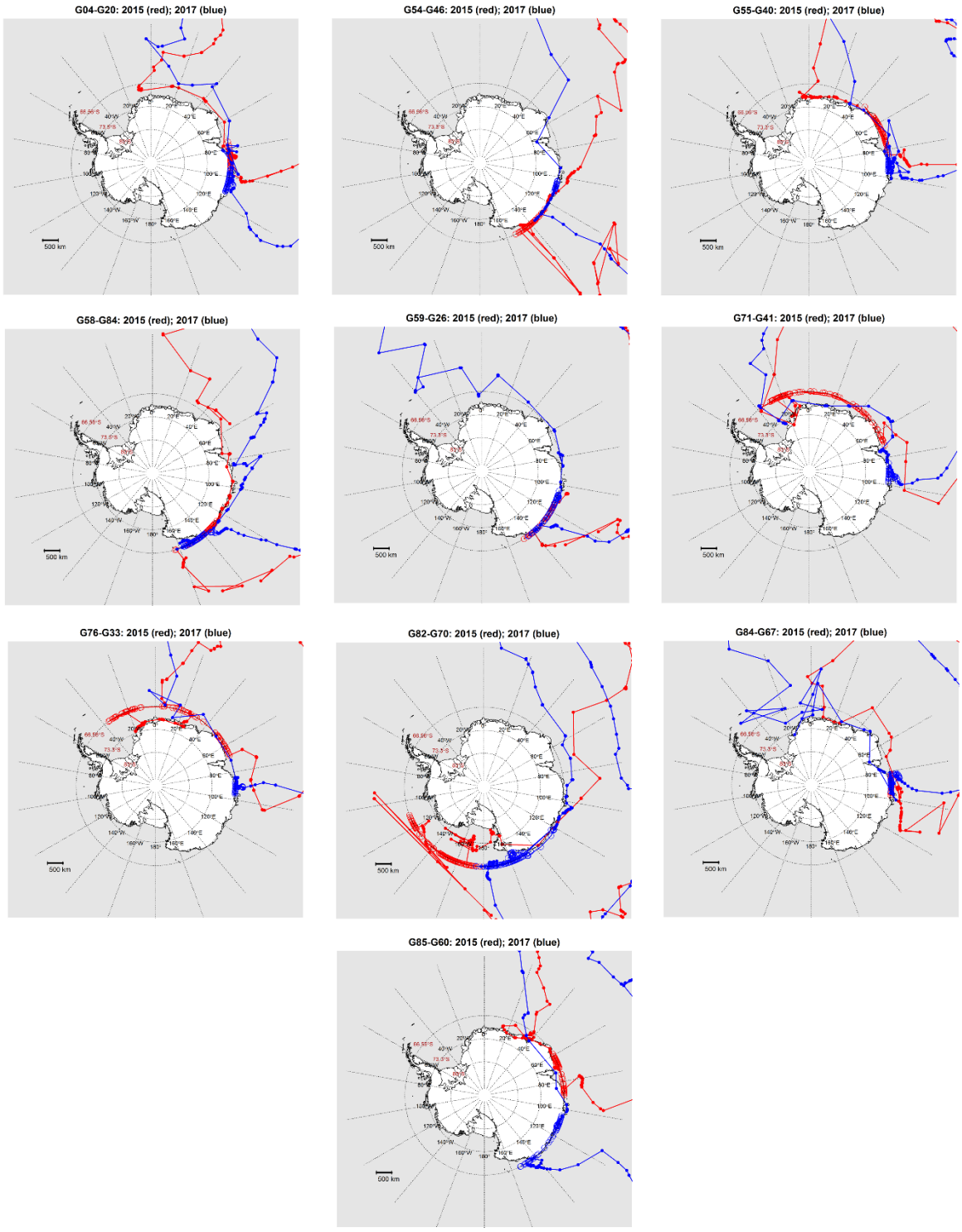

REFERENCES

Bestley, S., Raymond, B., Gales, N. J., Harcourt, R. G., Hindell, M. A., Jonsen, I. D., Nicol, S., Péron, C., Sumner, M. D., Weimerskirch, H., Wotherspoon, S. J. and Cox, M. J. 2018. Predicting krill swarm characteristics important for marine predators foraging off East Antarctica. - Ecography (Cop.). 41: 996–1012.

Brooks, M., Kristensen, K., Benthem, K. ,va., Magnusson, A., Berg, C., Nielsen, A., Skaug, H., Mächler, M. and Bolker, B. 2017. glmmTMB Balances Speed and Flexibility Among Packages for Zero-inflated Generalized Linear Mixed Modeling. - R J. 9: 378-400.